IEICE TRANS. FUNDAMENTALS, VOL.E96–A, NO.10 OCTOBER 2013

PAPER

Effects of Channel Features on Parameters of Genetic Algorithm for MIMO Detection

Kazi OBAIDULLAH[†], **Constantin SIRITEANU**[††], *Nonmembers*, **Shingo YOSHIZAWA**[††*], *Member*, *and* **Yoshikazu MIYANAGA**[††a)], *Fellow*

SUMMARY Genetic algorithm (GA) is now an important tool in the field of wireless communications. For multiple-input/multiple-output (MIMO) wireless communications system employing spatial multiplexing transmission, we evaluate the effects of GA parameters value on channel parameters in fading channels. We assume transmit-correlated Rayleigh and Rician fading with realistic Laplacian power azimuth spectrum. Azimuth spread (AS) and Rician K-factor are selected according to the measurement-based WINNER II channel model for several scenarios. Herein we have shown the effects of GA parameters and channel parameters in different WINNER II scenarios (i.e., AS and K values) and rank of the deterministic components. We employ meta GA that suitably selects the population (P), generation (G) and mutation probability (p_m) for the inner GA. Then we show the cumulative distribution function (CDF) obtain experimentally for the condition number C of the channel matrix $\mathbf{H}$. It is found that, GA parameters depend on the channel parameters, i.e., GA parameters are the functions of the channel parameters. It is also found that for the poorer channel conditions smaller GA parameter values are required for MIMO detection. This approach will help to achieve maximum performance in practical condition for the lower numerical complexity.

key words: *Azimuth spread, condition number, correlation, fading, genetic algorithm, K-factor, Maximum likelihood, Meta GA, MIMO, WINNER II*

1. Introduction

Multiple-input/multiple-output (MIMO) wireless communications system has employed to improve performance over fading channels. MIMO system can provide higher bit rates and smaller error rates and therefore, predict tremendous performance gains over the conventional SISO concepts [1]. Spatial multiplexing techniques transmit information sequence independently over multiple transmit antenna without requiring additional bandwidth or transmission power. Thus, MIMO spatial multiplexing promises to generate a data-rate increase proportional to the minimum of the number of transmit and receive antenna [1]–[3].

However, the actual gains achievable in practice can be much smaller especially for unsuitable channel propagation conditions [4]. Nevertheless, the conventional MIMO detection techniques, e.g., maximum-likelihood (ML), matched filter (MF), zero-forcing (ZF) and minimum mean square error (MMSE), do not account for condition number (the ratio of the largest to the smallest singular values of the channel matrix with the fading gains) [5]. The condition number C for MIMO system is calculated from the instantaneous channel matrix $\mathbf{H}$. The channel is called *well conditioned* if a small error of the matrix coefficients results in small error of the solution and the reverse process is called *ill conditioned* channel.

Previous work on GA for MIMO [6]–[8] detection has not considered the effects of GA parameters, i.e., population size (P) and generation number (G) which determine the GA computational complexity on channel parameters, i.e., AS and K different propagation scenarios and deterministic ranks which determine Rayleigh and Rician fading channels.

Therefore, this paper shows by CDF how the channel fading assumption and parameters influence the required P and G values in different channel fading conditions. Since the ranges for these possible values are wide, the systematic searches for the best one is extremely complex. Genetic algorithms (GAs) implement evolutionary concepts [9] and have been shown feasible in finding solutions to optimization problems for the MIMO wireless systems [10], [11]. GA is able to overcome the user demand whereas conventional detectors are inefficient (poorer performance or higher complexity) [11]. The objective function (fitness function) of each individual, i.e., the value of individuals within the chromosome is determined according to [6], [11], which is based on the likelihood criterion.

To achieve higher probability, GA parameter requirements should be high. GA parameter requirements also depend on the number of antenna at the transmitter N_T. For higher probability, higher the N_T larger the GA parameter. A larger GA parameter increase is required when increase N_T. This is because the length of the individual greatly enlarges the search spaces. In our work we have considered $N_T = 4$.

Our simulation results are based on the WINNER II channel models. WINNER II has produced a valuable set of realistic MIMO channel models [13] and acts against the limitations of conventional channel models. Since AS and K plays an important role for MIMO wireless system performance [1] so one should use instead accurate AS and K values which have recently become available in [13]. WINNER II has modeled AS and K as lognormal distributions with scenario-dependent mean, variance and correlation. These

Manuscript received October 1, 2012.
Manuscript revised March 27, 2013.

[†]The author is with Rajshahi University, Rajshahi, Bangladesh.
[††]The authors are with the Graduate School of Information Science and Technology, Hokkaido University, Sapporo-shi, 060-0814 Japan.
[*]Presently, with Kitami Institute of Technology, Kitami-shi, 090-0015 Japan.
a) E-mail: miya@ist.hokudai.ac.jp

DOI: 10.1587/transfun.E96.A.1984

models also propose a Rician distribution for both the channel fading line of sight (LOS) and non-LOS (NLOS) propagation.

A Meta (outer) GA [12] is employed instead in order to evaluate the statistics of the required GA parameter values. In this paper, Meta GA searches for the most suitable values for the inner GA. This approach is new and exploited merely as a tool to reveal how the statistic of the required GA parameters are influenced by the MIMO channel statistic. Therefore, this contribution can help to find the complexity cost in different channel propagation scenarios/environments. Thus, GA-based MIMO detection of spatial multiplexing transmission is able to define the relation between GA parameter and channel parameter.

Our numerical results are based on the following:
• Rayleigh and Rician fading (various ranks of the channel matrix mean) with Laplacian power azimuth spectrum (PAS).
• AS and K values set by the means of the lognormal distributions (average and random) and correlation obtained by the WINNER II [13] for several relevant scenario types.

The related studies (previous work on GA) have also not explore the optimum GA parameters as for advanced (WINNER II) MIMO channel conditions. This paper has explored the optimum GA parameters for various channel conditions.

Simulation results have shown in Sect. 6, we have found that GA parameters depend on the channel parameters and GA complexity differs with various channel conditions according to their performance (poorer the performance lower the complexity or vice versa).

GA parameters are the function of the channel parameters which is a new step for GA-based MIMO detection in the wireless communications.

In this paper, scalars, vectors and matrices are represented by lower case italics, lowercase boldface and uppercase boldface, respectively. Further, $(\cdot)^H$ and $(\cdot)^\tau$ stands for Hermitian transpose and transpose operation, respectively, $[\cdot]_{i,j}$ indicates the i, jth element of a matrix, $\|\cdot\|$ denotes the norm of a vector, P stand for set of trial solution, gene represents a certain value set (bit) and alleles indicate the value of the gene (zero or one).

The rest of this paper is organized as follows. Section 2 introduces the models of the transmit signal, fading channel, receiver noise as well as the AS and K-factor. Section 3 describes conventional ML MIMO detection approach. Section 4 describes GA-based MIMO detection. Section 5 shows meta GA approach. Finally, Section 6 shows numerical results by using MATLAB [15].

2. System Model

2.1 Signal, Channel and Noise Models

Figure 1 shows the MIMO spatial multiplexing wireless communications system. We consider a frequency-flat

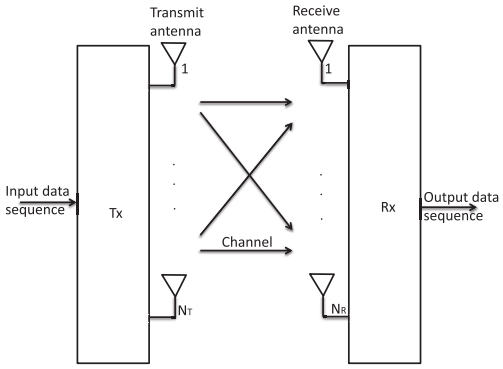

Fig. 1 MIMO spatial multiplexing.

Rayleigh and Rician fading MIMO channel with N_T transmit antennas and N_R receive antennas. Herein, we assume that $N_R \geq N_T$. For the numerical results shown later in this paper, each component of $\mathbf{x}$ is drawn from an Q-PSK modulation constellation. The complex-valued signal vector $\mathbf{x} = [x_1\ x_2 \ldots x_{N_T}]^\tau$ is transmitted from the base station an $N_T \times 1$. Therefore, the $N_R \times 1$ signal vectors received at the mobile station can then be written as [1]

$$\mathbf{y} = \sqrt{\frac{E_s}{N_T}}\mathbf{H}\mathbf{x} + \mathbf{n}. \tag{1}$$

In Eq. (1), E_s is the total transmit energy and $\frac{E_s}{N_T}$ is the energy transmitted per antenna, $\mathbf{H}$ is the $N_R \times N_T$ complex value channel matrix with the channel fading gains $|[\mathbf{H}]_{i,j}|$. It is assumed perfectly known and the noise vector $\mathbf{n}$ is the zero mean circularly symmetric complex Gaussian with variance $N_0 \times I_{N_T}$. The channel matrix $\mathbf{H}$ rows, their deterministic and their scatter components are denoted by $h_i = [h_1\ h_2 \ldots h_{N_R}]$, $h_{d,i} = [h_{d,1}\ h_{d,2} \ldots h_{d,N_R}]$ and $h_{r,i} = [h_{r,1}\ h_{r,2} \ldots h_{r,N_R}]$, respectively, for $i = 1 : N_R$. We assume that $h_{r,n,i}$ are independent with identical distribution $h_{r,n,i} \sim \mathcal{N}_c(0, \mathbf{R}_T)$, then h_i are uncorrelated with distribution $h_i \sim \mathcal{N}_c(h_{d,i}, \mathbf{R}_{T,K})$ with $N_T \times N_T$ covariance matrix $\mathbf{R}_{T,K} = \frac{1}{K+1}\mathbf{R_T}$ (when $K \neq 0$, $\mathbf{R}_{T,K} = 1/(K+1)\mathbf{R}_T$ and for $K = 0$, $\mathbf{R}_{T,K} = \mathbf{R}_T$). Therefore, the Gaussian matrix $\mathbf{H}_{r,n} = \mathbf{H}_{w,r,n}\mathbf{R}_T^{1/2}$ ($\mathbf{R}_T^{1/2}$ is the decompose form of Hermitian matrix $\mathbf{R}_T$ and $\mathbf{H}_{w,r,n}$ are Rayleigh channel components) with independent $[\mathbf{H}_{w,r,n}]_{i,j} \sim \mathcal{N}_c(0, 1)$.

The widely-recognized European WINNER II project has shown in [13] that measured $\mathbf{H}$ is a combination of a deterministic (i.e., mean) component (due to specular propagation) and a stochastic (i.e., random) component (due to diffuse propagation), i.e., $\mathbf{H} = \mathbf{H}_d + \mathbf{H}_r$. $\mathbf{H}_{d,n}$ and $\mathbf{H}_{r,n}$ are the normalized value of $\mathbf{H}_d$ and $\mathbf{H}_r$, respectively, i.e., $\|\mathbf{H}_{d,n}\|_F^2 = N_T N_R$ and $\mathbb{E}|[\mathbf{H}_{r,n}]_{i,j}|^2 = 1$, $\forall_{i,j}$ and then $\mathbb{E}\|\mathbf{H}_{r,n}\|_F^2 = N_T N_R$ and $\mathbf{H}$ is properly normalized. In terms of normalized components, the channel matrix can be written as [1], [4]:

$$\mathbf{H} = \sqrt{\frac{K}{K+1}}\mathbf{H}_{d,n} + \sqrt{\frac{1}{K+1}}\mathbf{H}_{r,n}. \tag{2}$$

where K is the Rician K-factor and is the power ratio of the deterministic and the random components of the channel

gain matrix are shown in (3) [4]:

$$\frac{\|\mathbf{H}_d\|_F^2}{\mathbb{E}|\mathbf{H}_r]|_F^2} = \frac{\frac{K}{K+1}\|\mathbf{H}_{d,n}\|_F^2}{\frac{1}{K+1}\mathbb{E}\|\mathbf{H}_{r,n}\|_F^2} = K. \quad (3)$$

We assume that $[\mathbf{H}]_{i,j}$ are complex-Gaussian distributed. Then, for $K = 0$ the term $\mathbf{H}_d = 0$ and then $\mathbf{H} = \mathbf{H}_r = \mathbf{H}_{r,n}$. Therefore, the fading gains $|[\mathbf{H}]_{i,j}|$ are purely Rayleigh distributed. For $\mathbf{H}_d$ nonzero channel mean, i.e., $K \neq 0$, and the elements of $\mathbf{H}_r$ are complex-valued. Gaussian random variables $[\mathbf{H}]_{i,j}$ has a Rician distribution and can model most measured scenario [14]. For $K = \infty$, the channel is non-fading (IID). Our simulation results are shown in Sect. 6 for IID, Rayleigh and Rician fading. For Rician fading, we assume that $r = 1$, N_T. For Rayleigh fading, $r = 0$ because $\mathbf{H}_d = 0$ which is the only rank-zero matrix. We also assume correlation at the transmit side and no receive correlation. Thus, the elements on each row of $\mathbf{H}$ are correlated but the elements on each column are not.

The performance of the multi-antenna system depends on the antenna geometry and channel condition that determines the rank $(\mathbf{H}_{d,n})$. Rank $(\mathbf{H}_{d,n}) = 1$ or N_T depends on the transmitter and receiver separation, D, as well as antenna elements separation x at the transmitter and receiver. For $(\mathbf{H}_{d,n}) = 1$ (outdoor scenario) $D \gg x$. In practice r is typically low [1]. On the other hand $(\mathbf{H}_{d,n}) = N_T$ (indoor scenario) D and x are similar.

2.2 Statistical models for AS and K-Factor

MIMO system performance depends on the AS and K values [1]. The AS is defined as the second central moment of the PAS, i.e., AS is the root mean square of the power azimuth spectrum (PAS) and determines the fading correlation. For the smaller AS, the received signals are highly correlated and the diversity gain is low. For higher AS, antenna correlation is low and therefore, the diversity gain is high [16]. For the numerical results shown in Sect. 6, we assume Laplacian PAS since it models well measured azimuthal power distribution and was also adopted in WINNER II.

Using thorough measurements the WINNER II project has modeled AS and K as lognormal random variables with scenario-dependent mean, variance and crosscorrelation as shown in Table 1, where $\chi, \psi \sim N(0, 1)$ and have correlation ρ [13], [17].

This table depicts the three WINNER II scenarios considered: 1) A1 (indoor) with mean AS of 56° and mean K of 7 dB; 2) B1 (urban microcell) with mean AS of 3° and mean K of 9 dB; and C2 (urban macrocell) with mean AS of 11° and mean K of 7 dB.

Table 1 Base-station AS and K statistics [13, Table 4-5].

Scenario	AS [°]	K	ρ
A1: indoor	$10^{1.64+0.31\chi}$	$10^{0.1(7+6\psi)}$	−0.6
B1: urban microcell	$10^{0.40+0.37\chi}$	$10^{0.1(9+6\psi)}$	−0.3
C2: urban macrocell	$10^{1.00+0.25\chi}$	$10^{0.1(7+3\psi)}$	+0.1

3. ML Detection

ML is a nonlinear optimum MIMO detection criteria [1]. For given $\mathbf{H}$, the optimum (nonlinear) detection approach is to search all M^{N_T} candidate vectors [1], [8] for

$$\widehat{\mathbf{x}}_{ML} = \arg\min_{\mathbf{x}} \left\| \mathbf{y} - \sqrt{\frac{E_s}{N_T}}\mathbf{H}\mathbf{x} \right\|^2. \quad (4)$$

Where $\|\cdot\|_2$ denotes the norm-2 of a vector.

The ML detection solution is the signal vector that minimizes the distance between the received signal vector and the linear combination of the channel matrix and the tested signal vector. ML can perform well but may require higher complexity due to the exhaustive search [8].

4. GA Detection

GAs are numerical optimization algorithms and can implement evolutionary concepts to solve complex optimization problems. GA balances exploitative (i.e., covering the space by crossover and mutation) and explorative principles (i.e., choosing the best candidates by selection) to expeditiously optimize functions over large space. GAs are often employed to reduce the complexity of searching for solutions of multidimensional optimization problems. Therefore, GAs are feasible competitors in MIMO detection [6], [8].

Figure 2 shows the steps of a typical GA. Some stochastic operators, i.e., selection, crossover and mutation are used to find the better solution. It maintains a population P of candidate solutions, i.e., chromosomes or individuals. At every GA generation the current population of

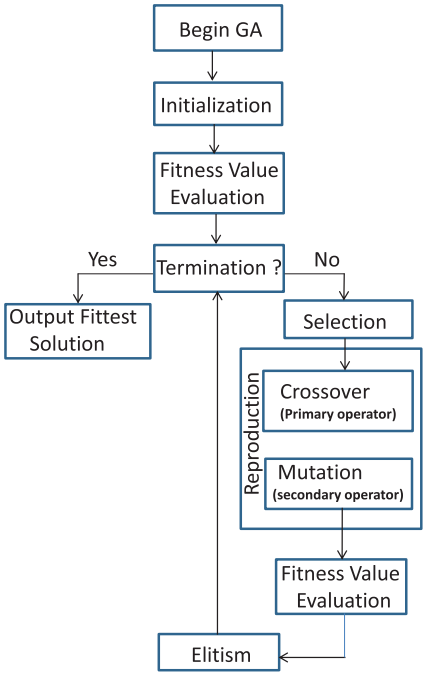

Fig. 2 Genetic algorithm diagram.

candidate solutions is evolving into a new population as discussed next.

Proper initialization is an important factor for GA convergence [8]. First population, i.e., the set of trial solutions are generated at this stage. However, the results are given by GA initialized with P random individuals [18]. In our case GA population forms a $N_T \times P$ matrix. The columns in this matrix are candidate transmitted signal vectors $\mathbf{x}$.

Then, the following metric is used to determine the fitness of each individual $\mathbf{x}$ in the population:

$$d = \left\| \mathbf{y} - \sqrt{\frac{E_s}{N_T}} \mathbf{H}\mathbf{x} \right\|. \tag{5}$$

A smaller d indicates a fitter candidate solution. Fitter individuals (better genes) are more likely to be selected to produce offspring individuals.

For the next generation, parents are selected based on their fitness value calculated with (5). We use for the selection of the fitness-proportionate method [8]. This method is referred *roulette-wheel selection* [19], whereby the fitness of the parents determines the probability of their generating offspring.

Crossover is working as the primary operator to create new individual. We use uniform crossover. Uniform crossover allows for gene exchange at any position in the chromosome, i.e., each of the N_T positions. The gene exchange is typically allowed with a certain probability. Then, offspring individuals are formed by copying symbols from one parent to the other. It is chosen according to a randomly generated binary crossover mask of the equal length as the chromosomes [8].

Mutation acts as the secondary operator. It helps the algorithm converging to the global optimum instead of the local optimum. This operator is responsible for introducing fresh and missed alleles into the population. Random mutation change the components of offspring individuals with probability p_m. In our case, each symbol of an offspring individual is allowed to mutate into any other constellation symbol with mutation probability p_m.

The objective function of each individual is determined according to [6]. Elitism is employed in order to avoid discarding the best solutions by replacing the lowest-fitness offspring with the highest-fitness parent individual [20] in every generation. As a result, the search space is greatly developed.

Finally, GAs typically run for a predetermined number of iteration (generation) denoted by G. Termination criterion helps to decide that the GA will continue for searching or stop. Then, GA complexity is proportional with the product PG, i.e., GA complexity increases linearly in both the P and G [8].

5. Meta GA Approach

Meta GA discovers different settings for parameter tuning. It is possible to use another GA for tuning the parameter sets instead of setting all parameters through error and trial basis.

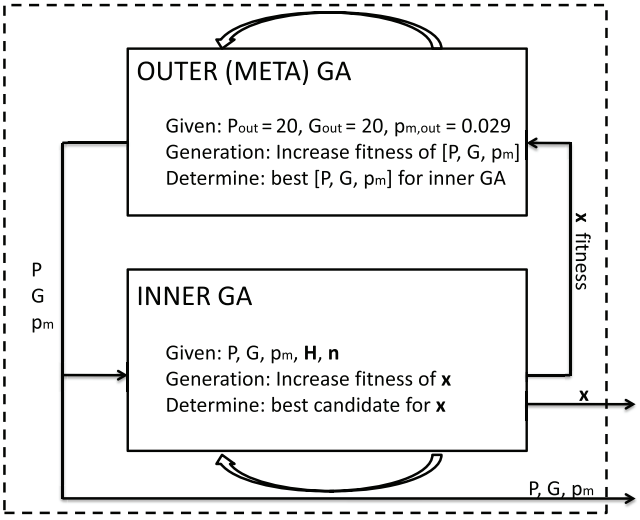

Fig. 3 Structure of employed algorithm.

That is why this GA is called Meta GA (outer GA) and it is comes from Greek word $\mu\epsilon\tau\alpha$. Meta GA targets automatic parameter calibration for the inner GA (inner GA parameter optimization). In our case, three variable optimizes are P, G and p_m. The advantages of the Meta GA is a small tuning time as a result and thus less with less computational complexity. It is attractive due to its automated search.

We employ Meta GA in order to determine the most suitable parameters for the inner GA which is then used to compare the effects of GA parameters on channel parameters. The structure is shown in Fig. 3. In some ranges of possible values for P, G and p_m, Meta GA has responsible for selecting the most suitable values for the inner GA. The outer GA generates the fittest triple [P, G, p_m] which is then employed by the inner GA. The inner GA then determines the fittest value of the transmitted signal vector, $\mathbf{x}$. Meta GA has an additional complexity but this complexity does not affect much for higher number of transmit antennas and for modulation constatation size.

To optimize outer GA we initialize the GA randomly.

The brief optimization process for Meta GA:

for g = 1 : 20 (g = generation outer GA)
if g == 1
fitness computation for outer GA (sort fitness P, G and p_m, 'descend')
——
best parents = best (:,1)
end;
evaluate selection, crossover and mutation ;
——
Obtained offspring;
fitness computation for offspring;
——
Elitism: replace worst child with best parent;
best(:, P) = best parents
re-sorting
——

return best parent (at each generation, if necessary)
best parents = best(:,1)
end
select the fittest of parameters

6. Numerical Simulation Results

6.1 Settings

We assume that $\mathbf{H}$ is perfectly known at the receiver, i.e., the receive correlation matrix is set to $\mathbf{I}_{N_R}$. Therefore, each column of $\mathbf{H}$ are uncorrelated. The correlation between the elements of each row of $\mathbf{H}$, i.e., the transmit correlation is then computed for a given AS value as mentioned in [21]. In the transmit-side PAS is set to the realistic Laplacian type, where the angle is set to $\theta_c = 5°$. In the figure, titles symbols 'a' and 'r' indicates that $\mathbf{H}_{w,r,n}$ is average over single sample and average over random samples (over the WINNER II AS and K distributions), respectively. According to Table [13, Table 4-5] AS and K have been generated for 10,000 samples. The value of r represents the rank of the channel matrix. The transmit and receive antennas are uniform linear arrays ($N_T = N_R = 4$) where inter element distance is equal to the half of the carrier wave length.

Each of the figure in the next subsection shows the results obtained from $N_s = 4096$ trials. The channel matrix $\mathbf{H}$, transmitted symbol vector $\mathbf{x}$ and receiver noise vector $\mathbf{n}$ are either the same or different from trial to trial. We have set $M = 4$ (i.e., QPSK) and $N_R = N_T = 4$. Scalar x is the antenna element separation, d indicates the fitter candidate solution and d is the deterministic components.

The outer GA population size, generation number and mutation probability has been set to $P_{out} = 20$, $G_{out} = 20$ and $p_{m,out} = 1/(P_{out}\sqrt{3}) = 0.029$. The GA has been initialized randomly.

The inner GA has been initialized randomly which is indicated with 'M0' in the figure titles and have shown in Sect. 6.2 following the notation from [8]. Selection is the fitness proportion method and fitness value is calculated by likelihood criterion [6]. The crossover operation employs the uniform approach but gene exchange is unrestricted (with a certain probability). For simplicity, incest is allowed but elitism is implemented.

In the presence of noise, the signal-to-noise ratio (SNR), i.e., E_s/N_0, is set to 20 dB mentioned in the figure titles. We have generated $2^{N_2} = 4096$ samples of the channel matrix, i.e., of the random components, $\mathbf{H}_{\mathbf{w},\mathbf{r},\mathbf{n}}$. Note that both N_2 and $N_s = 4096$ appear in the figure titles. Some of the figures title also display in full the total number of samples, i.e., $N_s = 2^{N_2} = 4096$.

We have generate $\mathbf{H}_{d,n}$ in the following way:

• For Rician fading with r = 1, $\mathbf{H}_{d,n}$ is generated as the outer product of the receive and transmit array steering vectors, i.e., $\mathbf{a}_R$ and $\mathbf{a}_T$, respectively. Their elements are given by $e^{-j\pi d_n \sin\theta_{d,R}(n_R-1)}$, $n_R = 1 : N_R$, (transmit signals are received at the receiver based on the number of receiving antenna) and $e^{-j\pi d_n \sin\theta_{d,T}(n_T-1)}$, $n_T = 1 : N_R$ (Signals are transmitted from the number of transmitting antenna), respectively, where d_n is the normalized interelement distance, i.e., $d_n = 1$, $\theta_{LOS,R} = \theta_{d,R} = 10°$ and $\theta_{LOS,T} = \theta_{d,T} = 5°$. Then, $\mathbf{H}_{d,n} = \mathbf{a}_R\mathbf{a}_T^{\mathcal{H}}$. Where $\theta_{LOS,R}$ and $\theta_{LOS,T}$ are the line of site (LOS) components of the receive and transmit antenna in the angular directions of $\theta_{d,R}$ (components to the receiver) and $\theta_{d,T}$ (components from the transmitter) respectively.

• For Rician fading $r = N_T$, $\mathbf{H}_{d,n}$ has been generated as a unitary matrix.

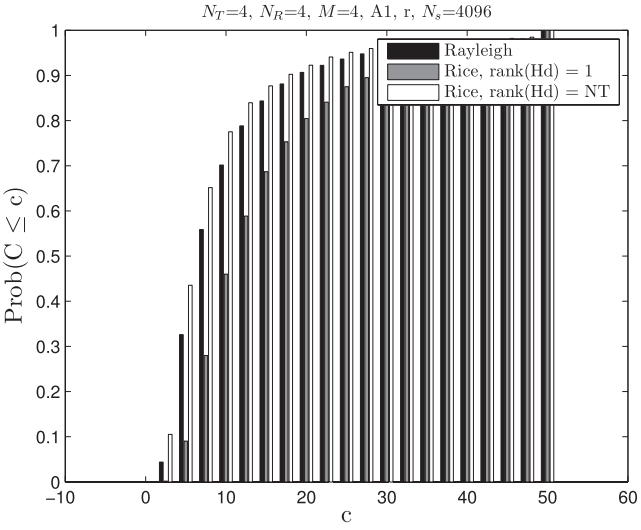

Fig. 4 CDF of C, for 4096 trials for scenario A1, and samples of $\mathbf{H}_{w,r,n}$, $\mathbf{x}$, $\mathbf{n}$.

6.2 Results and Discussion for Random $\mathbf{H}$ and $\mathbf{x}$, and $\mathbf{n}$

In this section, we considere the random samples of $\mathbf{H}_{w,r,n}$, $\mathbf{x}$ and $\mathbf{n}$. Smaller value of condition number implies a *well conditioned* channel matrix while large value indicates an *ill conditioned* channel matrix. In practice (i.e., $\mathbf{H}_d = 1$) channel is highly correlated. As a result condition number is high. Therefore, the condition number, i.e., the ratio of the largest to the smallest singular value ($\sigma_1 \geq \sigma_2 \geq \sigma_3 \geq \cdots \sigma_{N_T}$) for the employed sample of $\mathbf{H}_{w,r,n}$, was $C = 7.9$, 41.4 and 8.5, for $rank(\mathbf{H}_{d,n}) = 0$, 1 and N_T.

Figure 4 shows the CDF of the condition number C of $\mathbf{H}$ for Rayleigh fading as well as Rician fading with $rank(\mathbf{H}_{d,n}) = 1$ and $rank(\mathbf{H}_{d,n}) = N_T$. C tends to be largest for Rician fading with $rank(\mathbf{H}_{d,n}) = 1$ then for Rician fading with $rank(\mathbf{H}_{d,n}) = N_T$ and smallest for Rayleigh fading.

6.3 Results and Discussion for fixed $\mathbf{H}$ and $\mathbf{x}$, and $\mathbf{n} = \mathbf{0}$

In this section, we considere the single sample of $\mathbf{H}_{w,r,n}$, $\mathbf{x}$ and no $\mathbf{n}$. AS and K is WINNER II average. The outer GA has been executed repeatedly 4096 times for the same conditions, i.e., for the same sample of $\mathbf{H}_{w,r,n}$ (whose components were generated randomly and independently one time from a complex-value zero-mean and unit-variance Gaussian distribution) and $\mathbf{x}$.

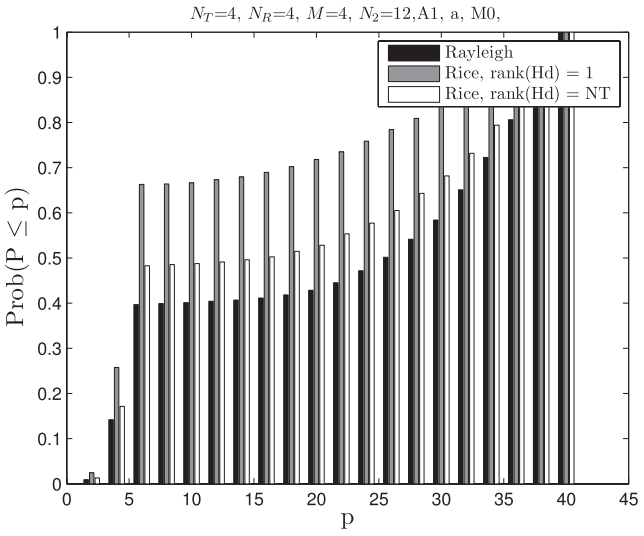

Fig. 5 CDF of P, for 4096 trials for scenario A1, and one sample of $\mathbf{H}_{w,r,n}$, $\mathbf{x}$, and no $\mathbf{n}$.

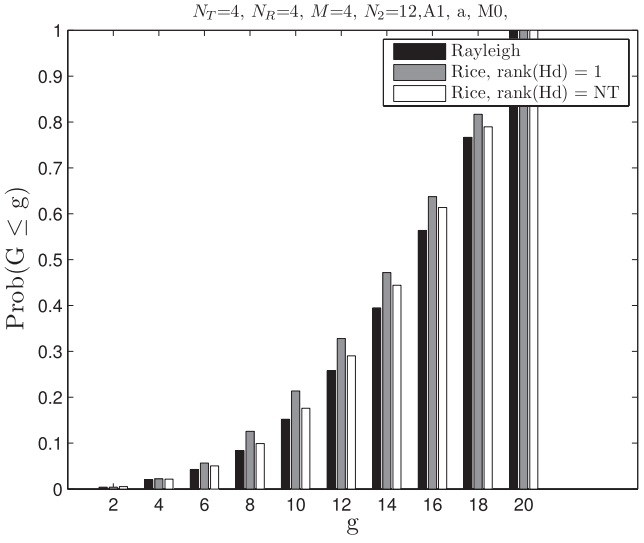

Fig. 6 CDF of G, for 4096 trials for scenario A1, and one sample of $\mathbf{H}_{w,r,n}$, $\mathbf{x}$, and no $\mathbf{n}$.

Figure 5 depicts the CDF of P values selected by the outer GA for the inner GA. Note that Rayleigh fading tends to require the largest P than by Rician fading with $rank(\mathbf{H}_{d,n}) = N_T$ and least for Rician fading with $rank(\mathbf{H}_{d,n}) = 1$.

Figure 6 depicts the CDF of G values selected by the outer GA for the inner GA. Rayleigh fading tends to require the largest G, followed by Rician fading with $rank(\mathbf{H}_{d,n}) = N_T$ and least G is required for Rician $rank(\mathbf{H}_{d,n}) = 1$.

From Fig. 5, it is observed that, for the same probability (0.7) the required population size for Rician rank 1 is 22 whereas required population for Rician full rank is 32 and Rayleigh is 34. Similar results (smaller scale) are also observed for the other figures in the same subsection. Meta GA approach reveals that the inner GA can be adapted to the channel condition. It achieves lower numerical complexity when the achievable performance is poor due to bad channel condition.

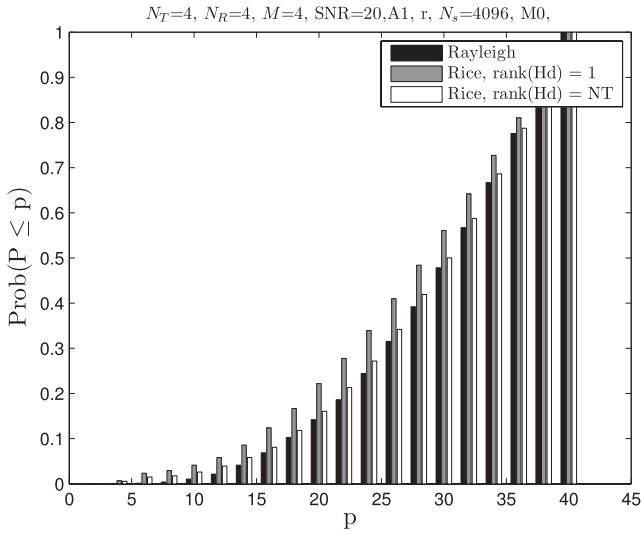

Fig. 7 CDF of P, for 4096 trials for scenario A1, and samples of $\mathbf{H}_{w,r,n}$, $\mathbf{x}$, $\mathbf{n}$, for $SNR = 20$ dB.

6.4 Results and Discussion for Random, Transmit-Correlated $\mathbf{H}$, $\mathbf{x}$ and $\mathbf{n}$ in Scenario A1

Figure 7 depicts the CDF of P values selected by the outer GA for the inner GA. AS and K set to WINNER II random (average over random AS and K values) for scenario A1. The elements of these matrices and vectors are all correlated. There is transmit (and always no receive) correlation.

Note that Rayleigh fading tends to require the largest P than Rician fading with $rank(\mathbf{H}_{d,n}) = N_T$. Rician fading with $rank(\mathbf{H}_{d,n}) = 1$ tends to require the smallest P.

Figure 8 depicts the CDF of G values selected by the outer GA for the inner GA. Note that the condition of $rank(\mathbf{H}_{d,n}) = 1$ requires the smaller G than $rank(\mathbf{H}_{d,n}) = N_T$ and highest for $rank(\mathbf{H}_{d,n}) = 0$.

Similarly, in Fig. 7 and Fig. 8, GA convergence is better, i.e., execution time is minimum for $r = 1$ (more realistic case) than $r = 0$ followed by $r = N_T$. All the results suggest that the condition of $r = 1$ offers an easer search space for the GA. The strong directionality of the search space for $r = 1$ appears to help faster GA convergence.

6.5 Results and Discussion for Random, Transmit-Correlated $\mathbf{H}$, Scenarios I.I.D., A1, B1, C2, Rician rank 1, and Random $\mathbf{x}$ and $\mathbf{n}$

Figure 9 depicts the CDF of P values selected by the outer GA for the inner GA. This section shows the results for 4096 trials each of which is for a different sample of $\mathbf{H}_{w,r,n}$, $\mathbf{x}$ and $\mathbf{n}$, i.e., the elements of these matrices and vectors are all correlated. A comparison of the CDF for P revealed that for Rician fading with $rank(\mathbf{H}_{d,n}) = 1$ it tends to be higher

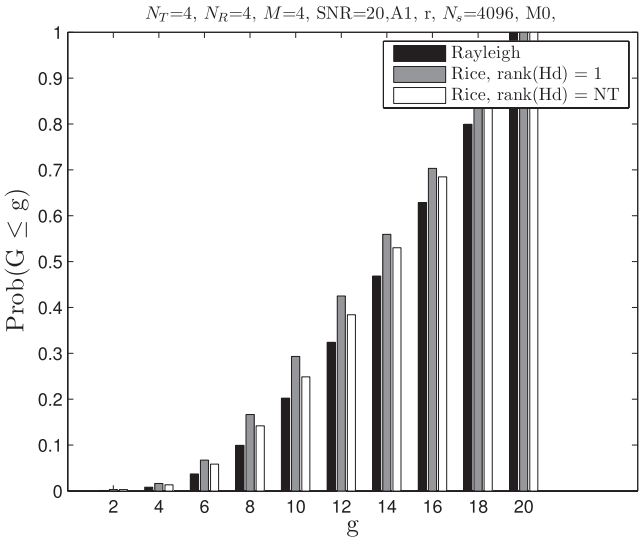

Fig. 8 CDF of G, for 4096 trials for scenario A1, and samples of $\mathbf{H}_{w,r,n}$, $\mathbf{x}$, $\mathbf{n}$, for $SNR = 20$ dB.

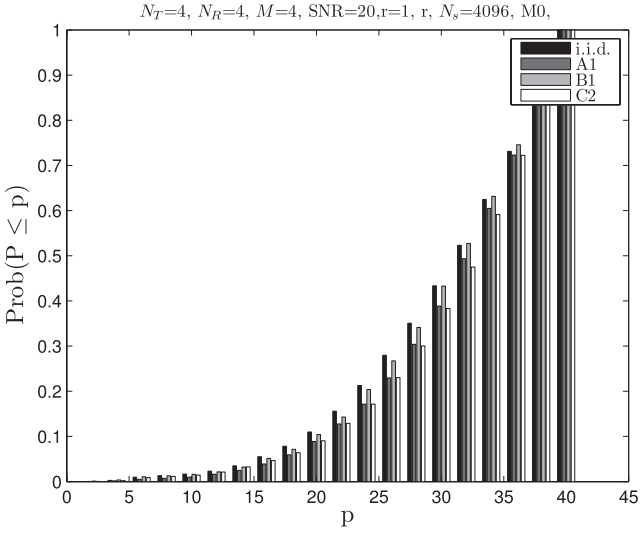

Fig. 9 CDF of P, for 4096 trials for scenario Scenarios I.I.D., A1, B1, C2, and random samples of $\mathbf{H}_{w,r,n}$, $\mathbf{x}$, and no $\mathbf{n}$, for $SNR = 20$ dB.

for scenario A1 and C2 than for scenario B1; P tends to be similar for B1 and i.i.d.

Figure 10 depicts the comparison of the CDF of G values selected by the outer GA for the inner GA and revealed that, for Rician fading with $rank(\mathbf{H}_{d,n}) = 1$ G tends to be similar for i.i.d., A1 and C2 but much higher than from B1. This is because a narrower power azimuth spectrum helps better 'steer' the GA within the search space. Results from Fig. 9 and Fig. 10 also suggest that GA parameters are affected by the channel parameters and narrower power AS spectrum offer an easer search space for GA convergence faster for bad scenario condition, when $rank(\mathbf{H}_{d,n}) = 1$.

We find that GA parameters are the function of the channel parameters. For different scenarios and different channel conditions GA parameter requirements are different.

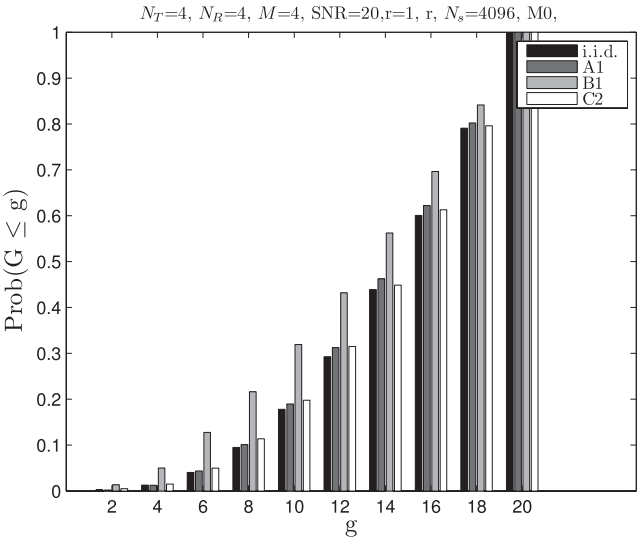

Fig. 10 CDF of G, for 4096 trials for scenario Scenarios I.I.D., A1, B1, C2, and random samples of $\mathbf{H}_{w,r,n}$, $\mathbf{x}$, and no $\mathbf{n}$, for $SNR = 20$ dB.

7. Conclusions

In this paper, we have evaluated the effects of channel parameter on GA parameter for MIMO detection in WINNER II channel model. It has shown that GA parameter depends on channel parameter. Using the meta (or outer) GA, we are able to show that the complexity of the inner GA that executes the MIMO detection can be adapted to the channel propagation conditions. GA complexity is lowest for the realistic case of Rician fading with lower rank of the channel matrix mean than Rician fading with large rank of the channel matrix mean and most complex for Rayleigh fading. Similarly, lower parameter values are required for the lower AS and higher parameter values are required for the higher AS. GA-based MIMO detection requires complexity proportional to the achievable performance, i.e., channel conditions that yield poorer performance require lower complexity whereas channel conditions that yield better performance require higher complexity.

Acknowledgement

The authors would like to thank the VLSI Design Education and Research Center (VDEC), Tokyo University for fruitful discussions. This study is supported in parts of Japan Science and Technology (JST) Agency A-STEP whose project title is "Design and Development of Ultra-Low Power High Speed Wireless communications LSI".

References

[1] A.J. Paulraj, R.U. Nabar, and D.A. Gore, Introduction to Space-Time Wireless Communications, Cambridge University Press, Cambridge, UK, 2005.

[2] A. Bonek, The MIMO radio channel, Institut fur Nachrichtentechnik und Hochfrequenztechnik, Technische Universitat Wien, Vienna, Austria, Tech. Rep., 2006. [Online]. Available: ernst.bonek@tuwien.ac.at
[3] J. Mietzner, R. Schober, L. Lampe, W.H. Gerstacker, and P.A. Hoeher, "Multiple-antenna techniques for wireless communication comprehensive literature survey," IEEE Communication Surveys and Tutorals, vol.11, no.2, pp.87–105, second quarter 2009.
[4] C. Siriteanu, X. Shi, and Y. Miyanaga, "MIMO zero-forcing detection performance for correlated and estimated Rician fading with lognormal azimuth spread and K-factor," IEEE Int. Conf. on Communications (ICC2011), pp.1–5, Kyoto, Japan, June 2011.
[5] S. Haene, D. Perels, and A. Burg, "A real-time 4-stream MIMO-OFDM transceiver: System design, FPGA implementation, and characterization," IEEE J. Selected Areas in Communications, vol.26, no.6, pp.877–889, 2008.
[6] G. Colman and T. Willink, "Overloaded array processing using genetic algorithms with soft-biased initialization," IEEE Trans. Vehicular Technology, vol.57, no.4, pp.2123–2131, July 2008.
[7] M.Y. Alias, S. Chen, and L. Hanzo, "Multiple-antenna aided OFDM employing genetic-algorithm-assisted minimum bit error rate multiuser detection," IEEE Trans. Vehicular Technology, vol.54, no.5, pp.1713–1721, Sept. 2005.
[8] M. Jiang and L. Hanzo, "Multiuser MIMO-OFDM for next-generation wireless systems," Proc. IEEE, vol.95, no.7, pp.1430–1469, July 2007.
[9] D.A. Coley, An Introduction to Genetic Algorithms for Scientists and Engineers, World Scientific Publications, Singapore, 1999.
[10] Y.G. Du and K.T. Chan, "Feasibility of applying genetic algorithms in space-time block coded multiuser detection systems," J. Digital Signal Processing, vol.15, no.2, pp.161–170, March 2004.
[11] S. Bashir, A.A. Khan, M. Naeem, and S.I. Shah, "An application of GA for symbol detection in MIMO communication systems," 3rd IEEE International Conference on Natural Computation (ICNC2007), 2007.
[12] K. Obaidullah, C. Siriteanu, S. Yoshizawa, and Y. Miyanaga, "Fading effects on parameter selection in genetic algorithm for MIMO detection," IEEE International Symposium on Intelligent Signal Processing and Communication Systems (ISPACS2011), pp.647–652, Chiang Mai, Thailand, Dec. 2011.
[13] P. Kyosti, J. Meinila, L. Hentila, et al., "WINNER II channel models," CEC, Tech. Rep. IST-4-027756, 2008.
[14] V. Erceg, L. Schumacher, and P. Kyritsi, "IEEE P802.11 wireless LANs. TGn channel models," May 2004.
[15] A. Czylwik and Y. Dhibi, "Matlab for communications," 9.3 MATLAB demonstration program visualizing the convolution procedure, Lab for Communications offered by the Department of Communication Systems of the University Duisburg-Essen.
[16] A. Algans, K.I. Pedersen, and P.E. Mogensen, "Experimental analysis of the joint statistical properties of azimuth spread, delay spread, and shadow fading," IEEE J. Selected Areas in Communications, vol.20, no.3, pp.523–531, April 2002.
[17] K. Obaidullah, C. Siriteanu, and Y. Miyanaga, "Performance and complexity of MIMO detectors for advanced wireless communications systems," IEICE Technical Report, SIS2011, pp.59–62, June 2011.
[18] L. Hanzo, L.-L. Yang, E.-L. Kuan, and K. Yen, Single and Multi-Carrier DSCDMA, John Wiley & Sons, IEEE Press, West Sussex, England, 2003.
[19] M.D. Maciej, J. Nawrocki, and A.H. Aghvami, Understanding UMTS Radio Network Modelling, Planning and Automated Optimisation, John Wiley and Sons, West Sussex, England, 2006.
[20] K. Yen and L. Hanzo, "Genetic algorithm assisted joint multiuser symbol detection and fading channel estimation for synchronous CDMA systems," IEEE J. Selected Areas in Communications, vol.19, no.6, pp.985–998, June 2001.
[21] C. Siriteanu and S.D. Blostein, "Maximal-ratio eigencombining for smarter antenna arrays," IEEE Trans. Wireless Communications, vol.6, no.3, pp.917–925, March 2007.

Kazi Obaidullah received his B.Sc. (Hons) and M.Sc. degrees in Applied Physics and Electronics from Rajshahi University, Rajshahi, Bangladesh in 1998 and 1999 respectively. Currently he is pursuing the Ph.D. degree at the Graduate School of Information Science and Technology, Hokkaido University, Japan. His research interests are in applying Artificial Intelligence (evolutionary intelligence algorithm) to Wireless Communication and Network Control Systems (NCS).

Constantin (Costi) Siriteanu received his B.S. and M.S. degrees in Electrical Engineering from Gheorghe Asachi Technical University, Iasi, Romania, in 1995 and 1996, respectively, and the Ph.D. degree from the Department of Electrical and Computer Engineering, Queens University, Kingston, Canada, in 2006, for work on adaptive signal processing for smarter antenna array receivers, with a focus on performance-complexity tradeoffs based on channel statistics. Since October 2009, he has been an Assistant Professor (research) with the Global Center of Excellence (GCOE) at the Graduate School of Information Science and Technology, Hokkaido University, Sapporo, Japan. His interests are in optimizing performance and energy consumption in wireless communications systems (with multiple antennas, feedback, cognitive concepts), improving the efficiency and safety of road trafic using communications and control, and in applying artificial intelligence algorithms to communication and control problems.

Shingo Yoshizawa received his B.Eng., M.Eng., and D.Eng. degrees from Hokkaido University, Sapporo Japan, in 2001, 2003, and 2005, respectively. He is currently an assistant professor of Laboratory of Information Communication Networks, Division of Media and Network Technology at the Graduate School of Information Science and Technology, Hokkaido University. His research interests are digital signal processing, speech processing, wireless communication systems and VLSI systems architecture.

Yoshikazu Miyanaga received his B.Eng., M.Eng., and D.Eng. degrees from Hokkaido University, Sapporo Japan, in 1979, 1981, and 1986, respectively. Since 1983 he has been with Hokkaido University. From 1984 to 1985, he was the visiting researcher at Department of Computer Science, University of Illinois, USA. He is currently a professor of Laboratory of Information Communication Networks, Division of Media and Network Technology at the Graduate School of Information Science and Technology, Hokkaido University. He served as an associate editor of IEICE Transactions on fundamentals of Electronics, Communications and computer science from 1996 to 1999, and editor of IEICE Transactions on Fundamentals, special issue. He is also an associate editor of Journal of Signal Processing, RISP Japan (2005 to present). He was a delegate of IEICE, Eng. Science Society Steering Committee from 2004 to 2006. He was a chair of IEICE TG-SIS during the same period and now a member of advisory committee, IEICE TG-SIS. He is served as a member in the bord of directors, IEEE Japan council and as a chair of student activities committee from 2002 to 2004. He is a chair of student activities committee in Sapporo section (1998–present). His research activities are in wide areas of, adaptive signal processing, non-linear signal processing, evolutionary algorithm, parallel/pipelined VLSI systems and speech signal processing.